American Journal of Science

THE EVOLUTION OF THE EARTH SURFACE SULFUR RESERVOIR

D. E. CANFIELD

Danish Center for Earth System Science (DCESS) and Institute of Biology, University of Southern Denmark, Campusvej 55, 5230 Odense M, Denmark; e-mail: dec@biology.sdu.dk

ABSTRACT. The surface sulfur reservoir is in intimate contact with the mantle. Over long time scales, exchange with the mantle has influenced the surface reservoir size and possibly its isotopic composition. Processes delivering sulfur to the Earth surface from the mantle include volcanic outgassing, hydrothermal input, and ocean crust weathering. The sulfide fixed in ocean crust as a consequence of hydrothermal sulfate reduction, and subduction of sedimentary sulfides, represent return pathways of sulfur to the mantle. The importance of these different pathways in influencing the size of the surface sulfur reservoir depends on the particulars of ocean and atmosphere chemistry. During times of banded iron formation when the oceans contained dissolved iron, sulfide from submarine hydrothermal activity was precipitated on the seafloor and subsequently subducted back into the mantle and, therefore, had little impact on the surface sulfur reservoir size. With sulfidic ocean bottom water conditions, which may have occurred through long stretches of the Mesoproterozoic and Neoproterozoic, significant amounts of sulfide is subducted into the mantle. When the oceans are oxic, sulfide subduction is unimportant, and an additional source, ocean crust weathering, delivers sulfur to the Earth surface. Thus, under oxic conditions the surface environment accumulates sulfur, and probably has for most of the last 700 million years.

Mass balance modeling suggests that the surface sulfur reservoir may have peaked in size in the early Mesoproterozoic, declined to a minimum in the Neoproterozoic, and increased to its present size through the Phanerozoic. The exchange of sulfur between the mantle and the surface environment can also influence the isotopic composition of the surface reservoir. Modeling shows that the subduction of ^{34}S-depleted sulfur through the Mesoproterzoic could have significantly increased the average δ^{34}S of the surface reservoir into the late Neoproterozoic. The preserved isotope record through the Neoproterozoic is well out of balance, with the average δ^{34}S for sulfate and sulfide both exceeding the modern crustal average. This imbalance could be explained, at least partly, if the crustal average was more ^{34}S-enriched than at present, as the modeling presented here suggests.

INTRODUCTION

Sulfur is an essential ingredient of life, and in oxidation states ranging from -2 to $+6$, it fuels the metabolism of countless different prokaryotic organisms, some of which evolved early in the history of life on Earth (Canfield and Raiswell, 1999). Microbial metabolism via sulfate reduction is of particular importance, contributing to around ½ of the carbon remineralization in coastal marine sediments (Jørgensen, 1982; Canfield, 1993). Pyrite (FeS_2) is an ultimate product of sulfate reduction, and its burial in sediments, and weathering on land, significantly influence the oxygen balance of the atmosphere (Garrels and Perry, 1974; Berner and others, 2000). The availability of sulfur to organisms and the magnitude of sulfur redox cycling will depend on the amount of sulfur available at the Earth surface and its oxidation state. This in turn should depend on the balance of sulfur exchange processes between the

Earth surface and the mantle. This balance, as will be explored in more detail below, depends on the details of ocean and atmosphere chemistry as they control the routes and the degree to which sulfur is exchanged between the mantle and the surface reservoir. Additionally, the isotopic composition of the whole surface reservoir can be affected if sulfur is exchanged with the mantle with an isotopic composition different from the average crustal reservoir. The reservoir exchange aspect of sulfur dynamics was explored by Hansen and Wallmann (2003) over the last 145 million years and is explored over much longer time scales here.

The purpose of the present contribution is to explore the long term evolution of the sulfur cycle over geologic time. Also explored are the isotopic consequences of this cycling, with an emphasis on the Neoproterozoic sulfur cycle which appears to be isotopically out of balance.

<center>the sulfur cycle</center>

Sulfur, in its principal forms as either pyrite (FeS_2) or gypsum ($CaSO_4 \cdot 2H_2O$) (with minor organic sulfur), is weathered from the continents as sulfate (SO_4^{2-}), and delivered to the oceans (fig. 1). Here, bacterial sulfate reduction reduces sulfate to sulfide, which can precipitate as pyrite in sediments, while seawater sulfate can also evaporatively precipitate as gypsum in isolated basins (Garrels and Perry, 1974; Berner and Raiswell, 1983). Over time these sulfur deposits become uplifted and exposed to weathering. The surface reservoirs are also connected to the mantle (Holser and others, 1988; Alt and others, 1989; Hansen and Wallmann, 2003), and three principal types of mantle sulfur input can be recognized (fig. 1). First, SO_2, with subordinate H_2S, outgasses from terrestrial volcanoes, mostly in convergent plate margins (Stoiber and others, 1987; Holser and others, 1988; Schlesinger, 1997; Halmer and others, 2002), but also from hot spot volcanics. This sulfur source is primarily of mantle origin (Sakai and others, 1982; de Hoog and others, 2001). However, the isotopic composition of basalts and associated gases from convergent margins can be quite enriched in $\delta^{34}S$ compared to the mantle (Kasasaku and others, 1999; de Hoog and others, 2001), implying a contribution also from sulfate in subducted marine sediment pore waters (de Hoog and others, 2001). Some subducted sedimentary pyrite might also contribute to the volcanic gas, but its contribution is minor compared to sulfate given the generally enriched $\delta^{34}S$ values of the volcanic gas. Estimates of the magnitude of this flux vary widely from low values of around 1×10^{11} mol yr^{-1} to high values of 14 mol $\times$ 10^{11} mol yr^{-1} (Stoiber and others, 1987; Holser and others, 1988; Schlesinger, 1997; Halmer and others, 2002). Most estimates tend towards the lower end of this range, with values most likely between about 1 to 3×10^{11} mol yr^{-1} of primary mantle sulfur (table 1).

Sulfide also vents to seawater as a result of subaqueous volcanism associated with ocean spreading centers (Von Damm, 1990; Elderfield and Schultz, 1996). The sulfur is released from hydrothermal fluids circulating through the volcanic system, and no more than 30 percent of this sulfur originates from seawater sulfate during hydrothermal circulation. The rest is from the mantle (Shanks and Seyfried, 1987; Von Damm, 1990). Estimates of this flux are obtained by combining vent fluid sulfide concentration with estimates of the water flux through the high temperature vents. Measured sulfide concentrations vary widely, and estimates of the magnitude of the sulfide flux range from 0.9 to 9.6×10^{11} mol yr^{-1} (Elderfield and Schultz, 1996).

Alternatively, estimates of sulfur exchange rates with the ocean crust are obtained from mass balance calculations on the isotopic compositions and concentrations of sulfur in sections of altered crust. Altered sections of crust show an upper region of sulfide removal. Some of the sulfur is lost during degassing of the basalts during crystallization and some by oxidative weathering of the volcanic rocks (Alt, 1994; Bach and Edwards, 2003). A lower zone of sulfide dissolution is also found within the
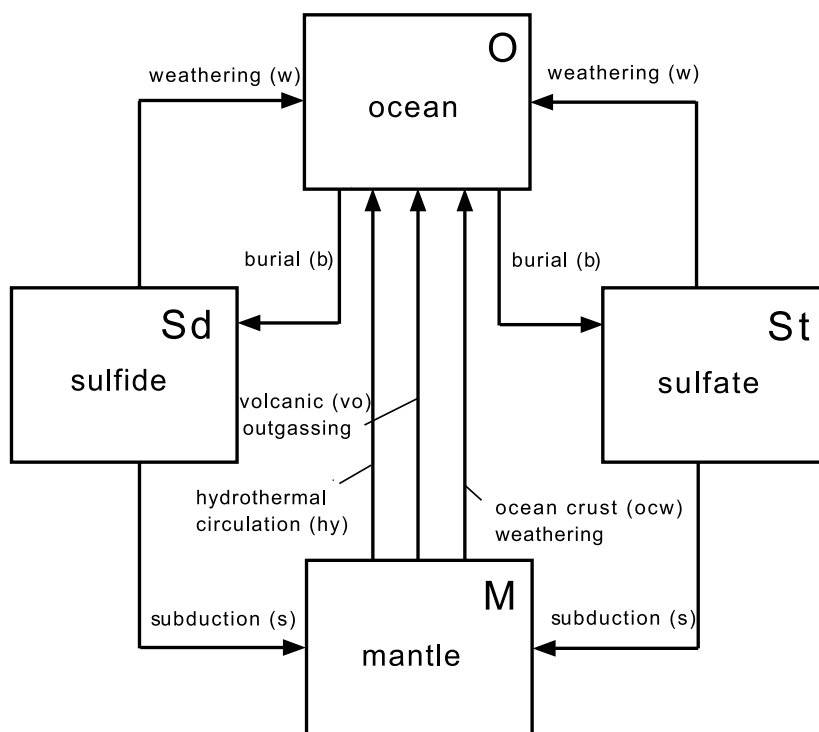
Fig. 1. A simplified version of the sulfur cycle is shown. The ocean (O) (also including the atmosphere) is the conduit through which sulfur transits. The sulfide reservoir (Sd) includes all sedimentary sulfides; both recently deposited and ancient, while the sulfate reservoir (St) includes seawater sulfate and sulfate evaporites. Both sulfate and sulfide are buried (b) from the ocean into the sulfide and sulfate reservoirs, which are subsequently uplifted onto land and exposed to chemical weathering (w), returning sulfur back to the oceans as sulfate. The boxes representing the ocean (O), sulfide (Sd), and sulfate (St) are the surficial reservoirs of sulfur. The surficial reservoirs are connected to the mantle (M) from which sulfur escapes by volcanic outgassing (vo), hydrothermal circulation through ocean spreading centers (hy), and the oxidative weathering of ocean crust (ocw) during off axis lower temperature hydrothermal circulation. Sulfur is returned to the mantle by the subduction of sedimentary sulfides formed during times of ocean anoxia (see text). Sulfides are also formed and fixed within the ocean crust during high temperature hydrothermal circulation where sulfate is inorganically reduced to sulfide. This transit path is shown from the sulfate box (St) into the mantle (M).

sheeted dike complex and the upper gabbro zone (Alt and others, 1989, 1995; Alt, 1994). In addition, there is a pronounced zone of secondary sulfide precipitation in the transition zone between the upper volcanic rocks and the sheeted dikes below. Some of this sulfur comes from sulfide released from the sheeted dikes, and some comes from the reduction of seawater sulfate deeper in the crust at high temperatures. In total, the dissolution and oxidation of ocean crust sulfides contributes about 0.8×10^{11} mol y^{-1} of sulfur to the oceans. This estimate is based on mass balance calculations of the Troodos ophiolite (Alt, 1994) and altered ocean crust off the Costa Rican coast (DSDP site 504B; Alt and others, 1989). A similar estimate of $1.1 \pm 0.7 \times 10^{11}$ mol y^{-1} is provided by Bach and Edwards (2003).

Of this total sulfur input, about equal amounts come from the upper pillow basalts and from the lower sheeted dikes and upper gabbros. Within the upper basalts, about ½ of the sulfur is lost, probably, from degassing during crystallization, and about ½ from oxidative weathering. The sulfur input flux calculated from crustal mass balance is at the lower end of the range determined from vent fluid chemistry. The reduction

<div align="center">

Table 1

Magnitude of present-day fluxes into and out of the mantle.

</div>

Flux	Magnitude $\times 10^{11}$ mol y^{-1}	ref
volcanic outgassing (M-O)[a]	1 to 3	1,2
hydrothermal input (M-O)	0.9 to 9.6	3
	0.6[b]	4,5
ocean crust weathering (M-O)	0.2	4,5
hydrothermal sulfate (St-M) reduction	0.4 to 0.9	4
sediment sulfide (Sd-M) subduction	3.6 to 9[c]	Present study

[a]see fig. 1 for key to letter designations.
[b]not including ocean crust weathering which is listed separately.
[c]potential rate when the oceans are sulfidic.
1, Stoiber and others (1987); 2, Holser and others (1988); 3, Elderfield and Schultz (1996); 4, Alt (1994); 5, Alt and others (1989).

of seawater sulfate during hydrothermal circulation and its precipitation in altered ocean crust is a sulfur sink into the mantle and will be considered in more detail below.

Sulfate is removed as anhydrite into ocean crust during high temperature hydrothermal circulation of seawater at ocean spreading centers (Alt and others, 1989). Most of the anhydrite is redissolved and returned to the ocean during lower temperature, off-axis circulation (Alt and others, 1989; Alt, 1994). As noted above, a small portion of the circulating sulfate is, however, reduced to sulfide, and some of this is fixed as solid phase sulfide minerals, forming a return path of sulfur back into the mantle (Alt and others, 1989). From the analysis of the sulfur and Fe chemistry of ocean basalts of a variety of ages Bach and Edwards (2003) conclude that Fe and sulfide in the upper pillow lavas might be more extensively oxidized than envisaged by Alt and others (1989). However, whether this oxidation influences the sulfide reduced during high temperature hydrothermal sulfate reduction is unclear. From Alt (1994) the rates of sulfide retention as a result of high temperature sulfate reduction are estimated at about 0.9×10^{11} mol y^{-1} for the Troodos ophiolite, and 0.4×10^{11} mol yr^{-1} for the DSDP hole 504B, and these estimates will be used here.

There is, in addition, the uptake of metal sulfides associated with microbial and thermochemical sulfate reduction in serpentinized ocean crust (Alt and Shanks, 1998), as well as some anhydrite precipitation. The magnitude of this flux is poorly constrained and probably lies somewhere between 0.13 to 1.9×10^{11} mol yr^{-1} (Alt and Shanks, 2003). Hence, it could be an important return route of sulfur back into the mantle. However, the modeling from Hansen and Wallmann (2003) suggests that the flux probably lies towards the lower end of the estimates, and in the modeling that follows sulfur removal associated with serpentinization will not be considered.

The subduction of pyritized marine sediments constitutes another potential return pathway for sulfur into the mantle. Most deep-sea sediments entering subduction zones are subducted into the mantle at an estimated Cenozoic average of 1.0 km^3 y^{-1} (von Huene and Scholl, 1991). Subduction erosion also removes crustal material into the mantle. During subduction erosion material from the upper overriding plate is eroded and entrained by the subducting slab (von Huene and Scholl, 1991). The material removed by subduction erosion is a complex mix of accreted sediment (in accretionary prisms) and crystalline rock. Overall, subduction erosion removes about 1.5 km^3 y^{-1} of material into the mantle (von Huene and Scholl, 1991).

As deep-sea sediments generally contain little pyrite today, the subduction of deep-sea sediments presently removes little pyrite into the mantle. There are no estimates of the pyrite content of material removed into the mantle by subduction erosion. However, crystalline crustal rock is likely to be pyrite poor, and much of the accreted sediment removed by subduction erosion is likely derived from the deep sea, which is also presently pyrite poor. Thus, overall, subduction is probably not today an important removal pathway of pyrite into the mantle. However, this would change during times of sulfidic ocean bottom water conditions as probably occurred during a substantial portion of the middle Proterozoic (Canfield, 1998; Shen and others, 2002, 2003; Arnold and others, 2004; Poulton and others, 2004), and also during isolated times in the Phanerozoic (Berry and Wilde, 1978). The magnitude of this sink is calculated from the subduction rate of terrigenous sediments into the mantle, estimated at between 1×10^{15} to 2.5×10^{15} g yr^{-1} (Hay and others, 1988; von Huene and Scholl, 1991). This sediment is assumed to have a total Fe content of 4 weight percent, and furthermore, about 25 percent of this Fe is assumed to be reactive toward sulfide, as is true for modern deep-sea sediments (Raiswell and Canfield, 1998). With these figures, a removal rate of total sulfide, as pyrite, into the mantle of between 3.6×10^{11} to 9×10^{11} moles yr^{-1} is obtained (table 1). This range of estimates could be viewed as a maximum removal rate of pyrite assuming the whole ocean deep-ocean floor is exposed to sulfide.

SULFUR CYCLE OVER GEOLOGIC TIME

In what follows, the evolution of the sulfur cycle will be considered from two different perspectives. Considered first is the isotope record of sulfide and sulfate over geologic time. From this record we can explore the relative burial histories of sulfate and sulfide as they pertain to the evolution of the oxidation state of the sulfur reservoir through time. A model reconstructing the size of the surface sulfur reservoir provides the second perspective of the evolution of sulfur cycle. Here, the processes controlling the inputs and outputs to the surface reservoir depend on the oxidation state of the atmosphere and oceans. It is shown that the size of the surface reservoir has been dynamic through Earth history. These perspectives combine when considering the isotope record in more detail, where important episodes of apparent isotope imbalance are found. This imbalance can be evaluated, at least in part, from the growth history of the sulfur reservoir as deduced from the model results.

The Isotope Record of Sulfur Cycle Evolution

The history of sulfide and sulfate removal from the oceans can be determined from the isotope record of sedimentary sulfides and seawater sulfate (Holland, 1973; Garrels and Lerman, 1981) using the following mass balance expression:

$$f_{py} = (\delta^{34}S_{in} - \delta^{34}S_{sul})/(\delta^{34}S_{py} - \delta^{34}S_{sul}), \qquad (1)$$

where f_{py} is the fraction of total sulfur removed from the oceans as pyrite (the remainder is as sulfate), $\delta^{34}S_{in}$ is the isotopic composition of sulfur weathered from the continents and delivered to the oceans, $\delta^{34}S_{sul}$ is the isotopic composition of seawater sulfate, and $\delta^{34}S_{py}$ is the average isotopic composition of pyrite sulfur removed from the oceans.

Over 3000 analyses of the isotopic composition of sedimentary pyrites through time have been compiled (Canfield, 1998, 2001) and these are calculated into averages for individual geological formations and further averaged over specific time periods. Through the Phanerozoic, averages have been calculated over individual geological periods, and three time slices of 0.54 to 0.6 Ga, 0.6 to 0.7 Ga, and 0.7 to 1.0 Ga were used for the Neoproterozoic. Through the remainder of the Precambrian, 300 million

year time slices have been used. The average isotopic compositions of individual geologic formations, and for specific time periods, are shown in figure 2A. Using period averages, and the isotopic composition of seawater sulfate through time (which is not well constrained through broad periods of the Precambrian; Strauss, 1993; Canfield, 1998, but as we shall see below, this uncertainty matters very little in calculating f_{py} in the Precambrian) (fig. 2A), f_{py} is calculated for the last 2.75 Ga assuming a constant $\delta^{34}S_{in}$ of 3 permil (Holser and others, 1988). It is likely that $\delta^{34}S_{in}$ has varied through time, and this will be fully explored in a latter section. Before 2.75 Ga, small and uncertain differences between $\delta^{34}S_{py,}$ $\delta^{34}S_{in,}$ and $\delta^{34}S_{sul}$, yield unreliable results, and these calculations have been abandoned. Uncertainty in the calculation of f_{py} reflects the standard deviations obtained from averaging together individual formation averages within specific time periods.

From these compilations a few general, but important, observations can be made. First, from the Archean through the Mesoproterozoic the average isotopic composition of sulfide straddles the present-day input $\delta^{34}S$ of 3 permil plus or minus about 3 permil (fig. 2A). During the Neoproterozoic, the average isotopic composition of sulfide increases dramatically and approaches the isotopic composition of sulfate. The average isotopic composition of sulfide drops sharply into the Phanerozoic, with decidedly negative $\delta^{34}S$ values by the Mesozoic.

As expected, when the isotopic composition of sulfide is near the isotopic composition of sulfate input to the oceans ($\delta^{34}S_{py} \approx \delta^{34}S_{in}$), pyrite burial is the dominant sulfur removal pathway. This follows directly from equation (1). Also from equation (1), when $\delta^{34}S_{py} \approx \delta^{34}S_{in}$ the isotopic composition of sulfate has little influence on the calculation of f_{py}. Overall, through the late Archean, the Paleoproterozoic, and the whole of the Mesoproterozoic, the isotope record is consistent with dominant pyrite removal from the oceans with little evidence for significant sulfate precipitation. Consistent with this, evidence for large sulfate deposits is generally absent in the Archean and in the early Proterozoic, and there are only a few Mesoproterozoic sulfate deposits of note (Grotzinger and Kasting, 1993) with sizes ranging from 10^9 to 10^{10} m^3. Although these deposits seem large, their size can only account for 10 to 100 years of sulfate input to the oceans at the present rate of 2×10^{12} mol yr^{-1} (Berner and Berner, 1996). They, therefore, represent only small amounts of sulfur removal. Some sulfate deposits have undoubtedly long since weathered away, but one can only speculate as to the magnitude of such deposits.

By about 0.8 Ga sulfate deposition becomes more pronounced, and some significant massive sulfate deposits are found, like those from the Amadeus Basin, northern Australia (Grotzinger and Kasting, 1993; Gorjan and others, 2000) and the Little Dal Group from the Mackenzie Mountains Supergroup of Canada, as well as the 0.75 Ga Shaler Group on Victoria Island, Canada. Despite this, sulfate deposition is not indicated in figure 2B. Indeed, during most of the Neoproterozoic, the calculation of f_{py} reveals impossibly high pyrite burial proportions (fig. 4A; see also Hayes and others, 1992; Gorjan and others, 2000). The nature of these high f_{py} values and the Neoproterozoic sulfur cycle in general will be considered in more detail in a later section.

It appears from the isotope record that significant deposition of sulfate from the oceans is mainly a phenomenon of the Phanerozoic (last 0.54 Ga) and particularly the last 0.3 Ga (fig. 2B). Increased deposition of sulfate would logically reflect increased levels of atmospheric oxygen in the late Precambrian (Berkner and Marshall, 1965; Knoll, 1992; Canfield and Teske, 1996) and more effective oxidation of surficial pyrite to sulfate, increasing the levels of sulfate in the ocean. Probably also contributory is the switch from sulfidic to oxic bottom waters (see below) reducing in the size of the sulfide sink and the magnitude of pyrite burial. Summarizing these points:
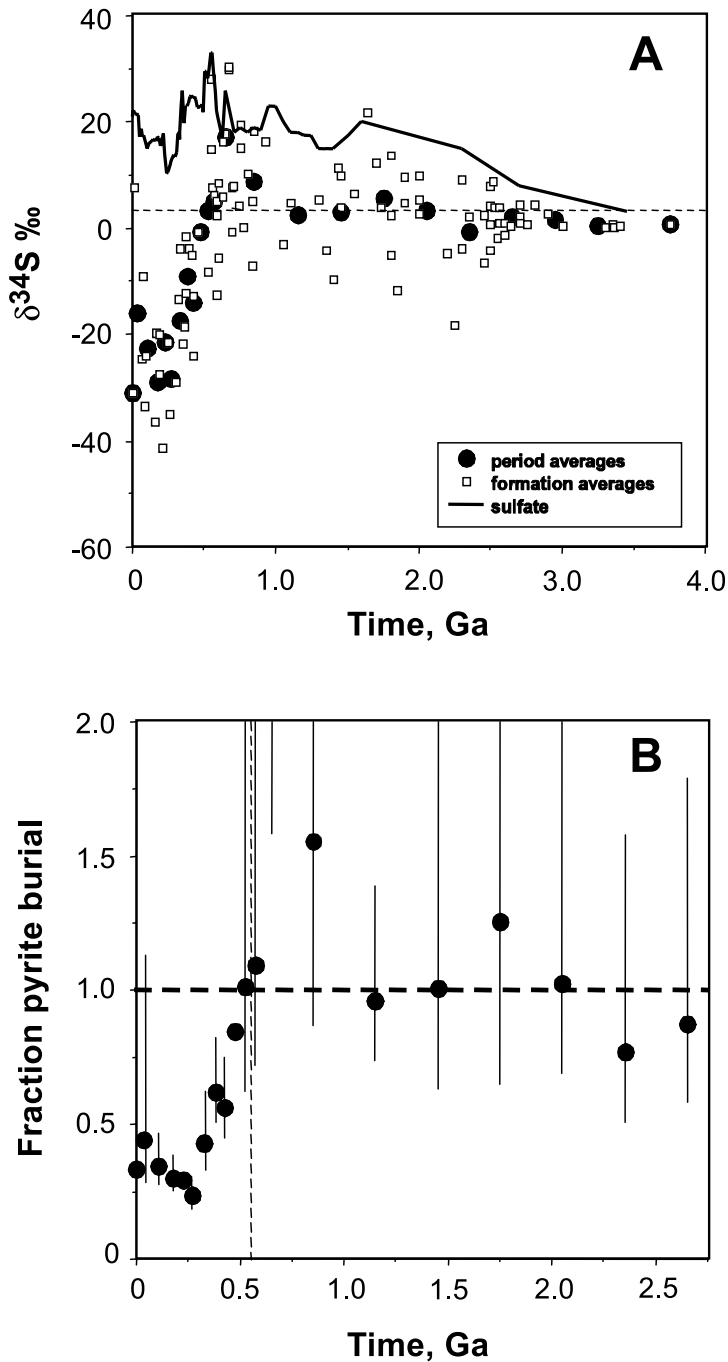
Fig. 2. (A) The isotopic composition of sedimentary sulfides is shown, averaged into formation averages, and period averages. Through the Phanerozoic, period averages represent the geologic periods. In the Neoproterozoic period averages represent the intervals 0.54 to 0.6 Ga, 0.6 to 0.7 Ga, and 0.7 to 1.0 Ga. Through the remainder of the Precambrian period averages were compiled for every 0.3 Ga. Also shown is the isotopic composition of seawater sulfate through time. Data are from Canfield (2001). (B) The fraction of total sulfur buried as pyrite is presented. This fraction is calculated from period averages utilizing equation (1). The error bars represent the standard deviation from period averages. Note that for the time interval 0.6 to 0.7 Ga the fraction pyrite burial (equal to 4.4) is off scale with only the bottom of the error bar showing.

1) There is little evidence for significant sulfate deposition in the Archean, Paleoproterozoic, and Mesoproterozoic, consistent with low levels of seawater sulfate at this time.
2) The sulfur cycle in the Neoproterozoic is apparently out of balance isotopically. A great deal of ^{34}S-depleted sulfide is missing from the record.
3) The first indication of significant sulfate precipitation is in the Phanerozoic in response to increasing atmospheric oxygen and subsequent increases in seawater sulfate concentrations, as well as a reduction in the extent of sulfidic ocean bottom water.

Evolution of the Earth-surface Sulfur Reservoir

The inventory of sulfur at the Earth surface includes sulfate in the oceans, as well as sulfate and sulfide in contemporary sediments and in sedimentary rocks preserved on the continents and in epicontinental settings. This inventory is controlled by the balance of sulfur fluxes into and out of the mantle. As proposed here, these fluxes have varied in intensity and direction in response to changes in ocean and atmospheric chemistry through time. In what follows, the history of ocean and atmosphere chemistry will be reviewed, and its influence on sulfur fluxes into and out of the mantle will be highlighted.

The substantial deposition of banded iron formations (BIFs) in the Archean and early Proterozoic indicates prolonged periods of deep iron-containing ocean water (for example, Holland, 1984) from which hydrothermally-derived sulfides would be immediately precipitated as iron sulfide minerals on the ocean floor. Most of this sulfide would be delivered back with the subduction of deep-ocean sediments and would have contributed little to the growth of the Earth surface sulfur reservoir. Atmospheric oxygen was also low (for example, Holland, 1994; Farquhar and others, 2000), and the deep ocean was anoxic, so no seafloor weathering of sulfide minerals was possible. Therefore, the only significant source of sulfur to the early Earth surface was the direct volcanic outgassing of SO_2 and H_2S to the atmosphere and surface waters. Seawater sulfate concentrations were also low, below 200 µM before about 2.4 Ga, and probably around 1 mM into the early Proterozoic (Habicht and others, 2002; Shen and others, 2002). Thus, the high temperature reduction of seawater sulfate at ocean spreading centers was not important. Persistent BIF formation occurred before 2.4 Ga and between about 1.8 Ga and 2.0 (Isley and Abbott, 1999).

There is no indication for significant BIF deposition between 2.0 and 2.4 Ga. The nature of deep-water chemistry during this time is therefore uncertain. Deep waters may have contained Fe, with the evidence thus far elusive, or they may have contained sulfide as suggested by Bjerrum and Canfield (2002). Alternatively, they may have been oxic. In what follows an Fe-containing bottom water is assumed, with the recognition that modeling should be revised as more information on early Proterozoic bottom water chemistry becomes available. A cartoon of the sulfur cycle prior to 1.8 Ga is shown in figure 3A.

Increasing ocean sulfate concentrations through the early Proterozoic to > 1 mM likely favored increasing rates of sulfide production by sulfate reduction, overwhelming iron delivery rates to the oceans by 1.8 Ga and causing the transition from iron-rich to sulfide-rich deep ocean water (Canfield, 1998). This condition may have lasted until late in the Neoproterozoic. Some accumulating observational data support this hypothesis. For example, extended periods (over hundreds of millions of years) of sulfidic bottom water are found in basinal settings within the Mesoproterozoic (Shen and others, 2002, 2003). Also, there is evidence for the transition from iron-rich to sulfide-rich bottom water in sediments just overlying the Gunflint Formation, representing one of the last early Proterozoic episodes of BIF deposition (Poulton and others, 2004). Also, from Mo isotope studies of sediments from the McArthur Basin, Arnold
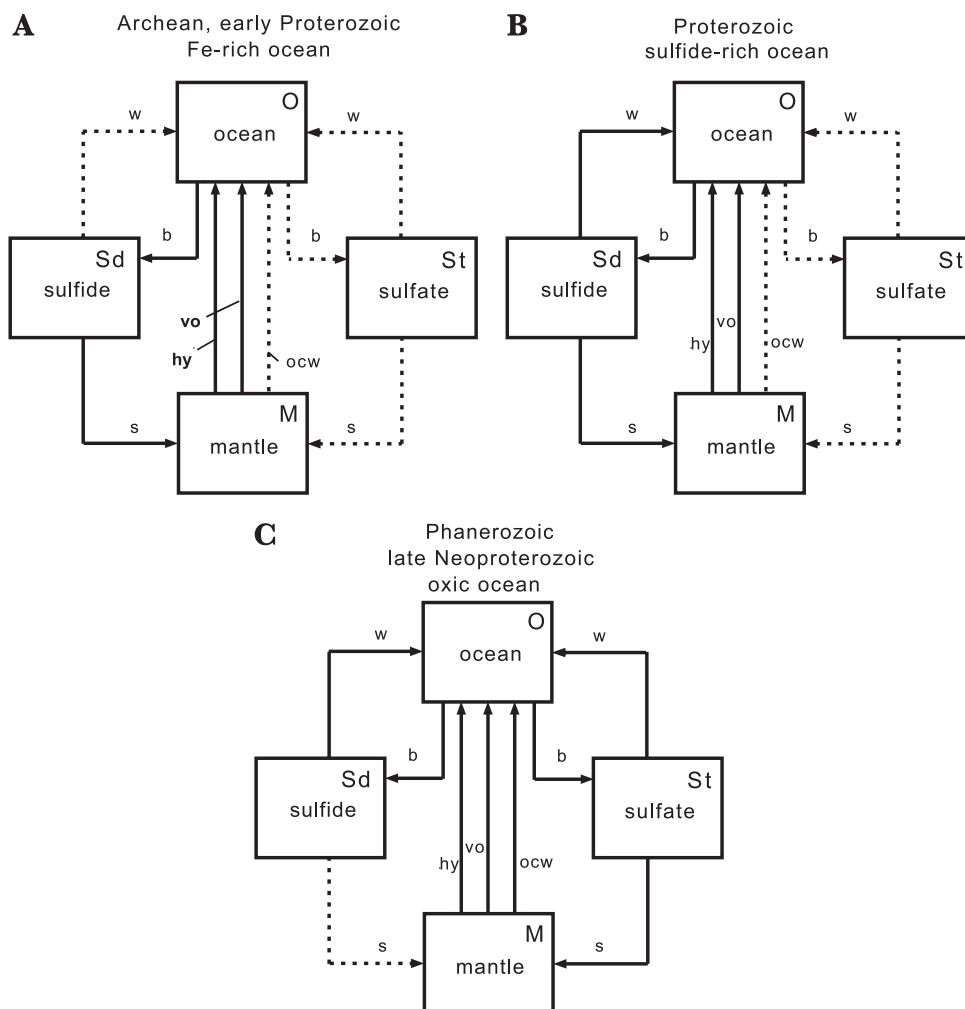
Fig. 3. The sulfur cycle is shown during different periods of Earth history. The dashed lines represent pathways that are either substantially suppressed or are inoperative with the particular conditions of ocean and atmospheric chemistry of the time: (A) the sulfur cycle during periods of the Archean and early Proterozoic, when the oceans were iron rich. During this period the sulfide subducted was mostly derived from hydrothermal sulfide inputs. Atmospheric oxygen was also low, (B) the sulfur cycle during periods of the Proterozoic when the oceans were sulfide rich. Here, the sulfide subduction rate is controlled by the subduction rate of reactive Fe-containing continental clastics, (C) the sulfur cycle during the last 0.7 Ga where the ocean was oxic. Sulfide subduction is suppressed without bottom water anoxia. See text and table 2 for further details. Symbols are the same as those in figure 1.

and others (2004) conclude that a substantial portion of the global ocean was sulfidic between 1.4 and 1.7 Ga. If the sulfidic middle Proterozoic ocean model is correct, the subduction of pyritized terrigenous deep-sea sediments was a significant sulfur removal pathway from the surface reservoir, and this pathway may have been important from 1.8 Ga to about 0.7 Ga. Furthermore, deep-water anoxic conditions would have inhibited seafloor weathering reactions, and relatively low ocean sulfate concentrations of probably around 2 mM, as inferred by Shen and others (2002), would have limited the high temperature inorganic reduction of seawater sulfate at mid-ocean

A summary of ocean chemistry and the presence or absence of mantle sulfur inputs and outputs over time.

Time period (Ga)	ocean chemistry	volcanic outgassing[e]	hydrothermal input	ocean crust weathering	hydrothermal sulfate reduction	sediment sulfide subduction[c]
4.5 to 1.8	Fe-rich	+[a]	-[b]	-	-	-
1.8 to 0.7	sulfide-rich	+	+	-	-	+
0.7 to 0	oxygen-rich	+	+	+	+[d]	-

[a]in some models the magnitude has been reduced to simulate the subduction of a portion of the input back into the mantle.

[b]all of the hydrothermal input is assumed to be subducted back into the mantle when this pathway is active.

[c]only includes the sulfide from the pyritization of terrigenous sediment particles when the ocean is sulfide rich.

[d]switched on at the Cambrian-Precambrian boundary (0.54 Ga) in light of evidence for low late Neoproterozoic concentrations of sulfate (see text).

[e]direct volcanic outgassing to the atmosphere and surface environment. Does not include hydrothermal flux at ocean spreading centers.

spreading centers. An outline of the sulfur cycle from about 0.7 to 1.8 Ga, with sulfidic deep-water, is shown in figure 3B.

Beginning around 0.7 Ga, at least periodic oxygenation of the deep ocean was likely (Canfield and Teske, 1996), and although several periods of deep-water anoxia existed in the Phanerozoic (for example, Berry and Wilde, 1978), it is assumed that over the last 0.7 Ga the deep ocean remained dominantly oxygen-rich, and sulfate-rich. As we shall see below, there was probably not a rapid increase in seawater sulfate concentrations at 0.7 Ga. Nevertheless, we assume a step function for simplicity in modeling. In switching to oxic ocean bottom waters, the removal of sulfur by the subduction of deep-sea sediments becomes negligible, and the oxidation of ocean crust during hydrothermal circulation provides a new source of sulfur to seawater. The only sulfur sink into the mantle is the incorporation of seawater sulfate, reduced to sulfide, and fixed in the ocean crust during high temperature hydrothermal circulation (see above). As mentioned above, sulfate reduction during serpentinization is another potential sulfate sink, but its magnitude may well be small and it is not considered here. A cartoon of the sulfur cycle over the last 0.7 Ga is shown in figure 3C.

Modeling Surface Reservoir Size

In the following model, the processes controlling the fluxes of sulfur to and from the mantle are regulated by ocean and atmosphere chemistry as described above and as summarized in table 2. Furthermore, rates of volcanic outgassing, hydrothermal input, ocean crust weathering, and the removal rate of sulfur from high temperature sulfate reduction are scaled with the history of heat flow from the Earth interior (Turcotte, 1980), which influences rates of tectonic activity. The model explores the scaling of these fluxes both linearly as a function of heat flow and as a function of heat flow squared. Plate velocity scales with heat flow squared if the mantle is modeled as a convecting layer with strongly heat-dependent viscosity (Gurnis and Davies, 1986). As some of the exchange processes may vary with plate velocity, a squared functionality is also explored. The history of heat flow is approximated relative to today (Q_{rel}) with equation (2), where t is time before present in Ga.

$$Q_{rel} = 1.00 + 0.1217t + 0.0942t^2. \qquad (2)$$

By contrast, the subduction rate of pyritized deep-sea sediment is held constant during those periods when the ocean was believed to have been sulfidic as discussed above. This rate depends on the delivery rate of terrigenous sediment to ocean basins by weathering, whose relationship to heat flow is indirect and uncertain. In any event, scaling this return flux with heat flow (numerous model simulations were performed doing this) has little effect on the model results presented below.

The model explores a range of present-day sulfur input rates. In particular, volcanic outgassing rates at both the high and low end of the estimates are used (see table 1), and hydrothermal input rates between 0.6 and 1×10^{11} mol yr^{-1} are used. These rates of hydrothermal input are low compared to the whole range of fluxes estimated from mid-ocean-ridge sulfide data but at the upper end are somewhat higher than the fluxes calculated from ocean crust mass balance. The fluxes chosen are probably a good compromise, particularly since the fluxes estimated from crustal balances are more direct and likely the most accurate. The rates of hydrothermal sulfate reduction are relatively well constrained from observations, and the present-day rates are not varied in the model. Also not varied is the present day rate of ocean crust weathering. Note, however, that these fluxes do scale with heat flow as outlined in table 3 and are only activated during times of permissive ocean and atmospheric chemistry as discussed above and summarized in table 2. As mentioned above, rates of sulfate reduction in serpentinization zones are not included but also not yet well constrained.

In some cases the model was amended so that SO_2 and H_2S from volcanic degassing were added to the surface reservoir at 20 percent of its input rate early in Earth history when the ocean was iron-rich. This 20 percent reduction is a qualified guess based on the likely aerial extent of the Precambrain ocean, and it reflects the reasonable assumption that volcanically derived SO_2 and H_2S, and their photolysis products (Farquhar and others, 2001; Pavlov and Kasting, 2002), will settle with high probability into the marine realm and incorporate into organic biomass or sedimentary sulfides. A large portion of this sulfur should be lost, depending on water-column redox conditions, by subduction back into the mantle. Indeed, Farquhar and others (2002) found evidence for subducted Archean marine sulfides as sulfur inclusions in diamonds with mass-independent sulfur isotope compositions. Such isotope signatures are typical for Archean sedimentary rocks (Farquhar and others, 2000). This reduction in volcanic gas input was not applied when the ocean was sulfidic, as the subduction rate of sulfur is controlled by the subduction rate of Fe and not the input rates of volcanic gases. This scalar was also not applied when the oceans were oxic, as in this case sulfur subduction is relatively unimportant and not a function of volcanic gas delivery rates.

After deciding on the starting parameters, the relationship of mantle exchange processes with heat flow, and the scalar for volcanic outgassing (0.2 or 1), the model was run forward in time (starting at 4.5 Ga with no sulfur in the surface reservoir), and the subduction rate of pyritized sediment was adjusted to recover the present-day sulfur inventory. The pyrite subduction rate is the only free parameter. A total of nine model runs were performed, and input parameters, as well as important output parameters are summarized in table 3. If the estimated range of sulfide subduction rates from table 2 is taken as a constraint, then five of the model runs produce acceptable results. Three of the models (cases 1, 4 and 6) require unrealistically high rates of pyrite subduction (based on the range of pyrite subduction rates calculated above) during times of sulfidic ocean conditions, while case 8 required unrealistically low rates. The history of the Earth surface sulfur reservoir for each of the acceptable model scenarios is shown in figure 4. Of these, case 7 is considered the least likely, as it assumes the accumulation of all of the volcanically outgassed sulfur in the surface environment, which, as discussed briefly above, is probably unrealistic.

TABLE 3

Scenarios for model analysis of sulfur reservoir size (all fluxes $\times$ 10^{11} mol y^{-1})

|	case 1	case 2	case 3	case 4	case 5	case 6	case 7	case 8	case 9
Fluxes									
Volcanic outgassing	1.5	1.5	1.5	3.0	3.0	3.0	1.0	1.0	1.0
Hydrothermal input	1.0	1.0	1.0	1.0	1.0	1.0	0.6	0.6	0.6
Ocean crust weathering	0.2	0.2	0.2	0.2	0.2	0.2	0.2	0.2	0.2
Hydrothermal sulfate reduction	0.7	0.7	0.7	0.7	0.7	0.7	0.7	0.7	0.7
Sulfide subduction	10.4	3.3	7.0	22.3	8.0	15.2	5.6	0.9	3.4
Control parameters									
Scalar for volcanic outgassing	1	0.2	0.2	1	0.2	0.2	1	0.2	0.2
Power by which heat flow is scaled	1	1	2	1	1	2	1	1	2
Selected results (x 10^{20} mol)									
Sulfur reservoir max (Precambrian)	9.8	2.1	4.9	19.6	3.9	9.8	6.5	-	3.3
Sulfur reservoir min	1.9	1.9	1.9	0.8	0.4	0.6	2.7	2.6	2.5
Total sulfur through surface reservoir	21.9	21.9	48.0	35.0	35.0	76.0	14.1	14.1	30.7
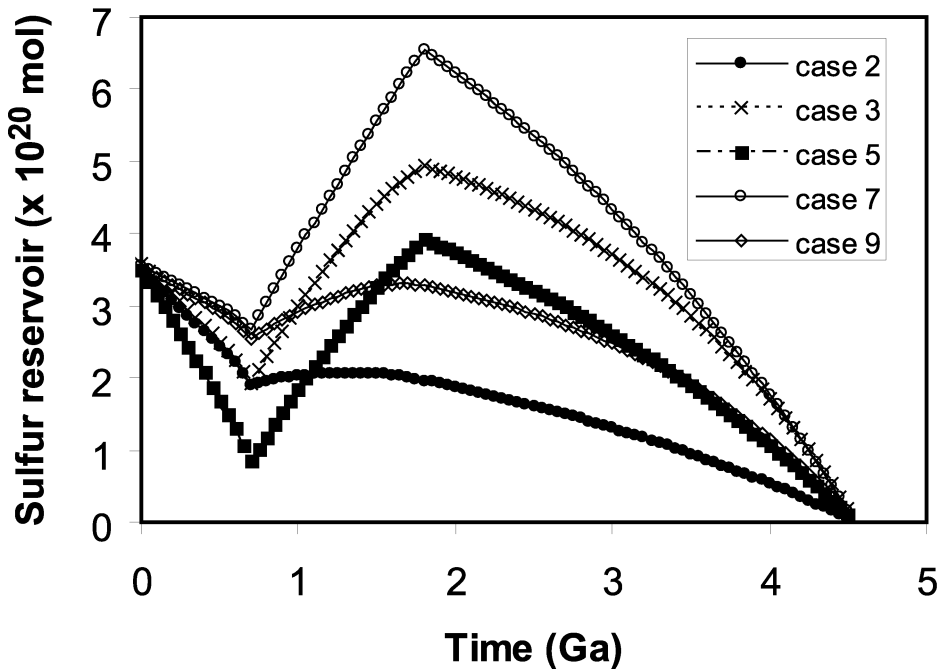
Fig. 4. The growth of the Earth surface sulfur reservoir for a variety of scenarios. These scenarios are not all of those explored, but those who meet the constraint imposed by the range of probable rates of pyrite subduction. See text and table 3 for details on the specific model parameters used in each case, and for a summary of important model output parameters.

All the most likely model results share features in common. In all cases, between 4 to 10 times the present sulfur inventory has been delivered to the Earth surface (table 3). This underscores the importance of sulfur return mechanisms to the mantle, in particular the subduction of pyritized marine sediments during times of sulfidic ocean conditions. Model results indicate that without this return mechanism the sulfur inventory would have been many times its present value. In all models (fig 4.), the sulfur inventory reached a Mesoproterozoic maximum, with the magnitude of the maximum depending on specific model conditions. Ignoring case 7, the most sulfur accumulation occurred either with a squared dependency of flux rates on heat flow (case 3), or with high estimates for present day hydrothermal and volcanic fluxes (case 5).

All models indicate a Neoproterozoic minimum in sulfur inventory size. The size of this inventory scales inversely with rates of sulfur input by volcanoes and hydrothermal sources. Thus, when sulfur input rates are high; the size of the minimum inventory is the lowest and vice versa. This relationship is rather non-intuitive, but the minimum inventory size results from a long period of sulfide subduction over the preceding ~1.1 Ga, and the magnitude of pyrite subduction flux varies positively with the strength of the volcanic sources. It follows that with high volcanic input a high pyrite subduction rate is required to recover the modern sulfur inventory. This process results in a high Mesoproterozoic sulfur inventory, and a low Neoproterozoic inventory. Because of a low Neoproterozoic inventory in most model runs, sulfur accumulates over the Phanerozoic under oxic bottom water conditions. During the Phanerozoic, the sulfur cycle is out of balance where the sources of sulfur to the surface environment outpace

the sinks back to the mantle by a sizable margin (table 1; see also Hansen and Wallmann, 2003).

Model results obviously depend on assumptions about the history of ocean and atmosphere chemistry, the magnitude of sulfur exchange fluxes with the mantle and how these scale with time. As there are potential uncertainties in all of these considerations, there is associated uncertainty in hindcasts of the history of the surface sulfur reservoir size. However, a broad range of input variables have been used here, and these allow the following rather robust generalizations:

1) Ocean and atmospheric chemistry have significantly influenced the size of the Earth surface sulfur reservoir by controlling the nature and magnitude of exchange fluxes between the mantle and the Earth-surface environment.

2) A substantial amount of sulfur has transited through the surface reservoir. In the models producing acceptable results, between 4 and 10 times the present surface sulfur inventory has been delivered to the Earth surface, emphasizing the significance of return paths of sulfur to the mantle, particularly by pyrite subduction.

3) It would seem that somewhere between and 60 percent to 140 percent of the present sulfur inventory accumulated by 1.8 Ga

4) The size of the surface reservoir likely reached a minimum in the Neoproterozoic, and the reservoir has grown substantially through the late Neoproterozoic and the Phanerozoic. This growth in the sulfur reservoir is almost inescapable. The oxygenation of the deep ocean removes the most significant sulfur sink, the subduction of pyrite, and introduces an additional sulfur source, the weathering of ocean crust. Indeed, with three significant sulfur sources, and one rather weak sulfur sink (table 1), the sulfur cycle is out of balance. This imbalance has occurred over 100's of millions of years.

The Neoproterozoic Sulfur Cycle

As mentioned above, the Neoproterozoic sulfur cycle appears to be out of balance isotopically, where the average isotopic composition of preserved sulfides approaches the isotopic composition of seawater sulfate. An excellent example comes from the 0.66 Ga marine Tapley Hill Formation from the Adelaide rift complex of South Australia (Gorjan and others, 2000; fig 5). Precipitated in the Tapley Hill are nodular and "chicken wire" anhydrites, which constrain the isotopic composition of the contemporaneous sulfate (fig. 5). The sulfides themselves show a range of values centered around the isotopic composition of sulfate. Similarly [34]S-enriched sulfides are also found in this time period in the Amadeus Basin, Australia, the Twitya Formation, Northwestern Canada, the Datangpo in China, and the Court Formation in Namibia (see summary in Gorjan and others, 2000). These results, therefore, support the observation that in many cases the average isotopic composition of sulfide is similar to that for sulfate.

One might argue that the preponderance of [34]S-enriched sulfides in the Tapley Hill and other similarly-aged deposits has somehow resulted from major, global scale, glaciations at around 0.7 Ga, just before the deposition of these sediments (Hoffman and others, 1998). If so, the relationship between the glacial events and the subsequent disruption of the hydrologic cycle, *et cetera*, on the generation of [34]S-enriched sulfides is not clear. This ambiguity is particularly true as the [34]S-enriched sulfides continue to form for the next 100 million years after the 0.7 Ga glacial episode. Indeed, even between 1.0 and 0.7 Ga, the deposition of [34]S-enriched sulfides was widespread (see fig. 2A, Gorjan and others, 2000), with no obvious relationship to glaciation. Thus, while global scale glaciations may have significantly influenced the sulfur cycle, the relationship between glaciation and the isotopic composition of sulfur species is unclear.
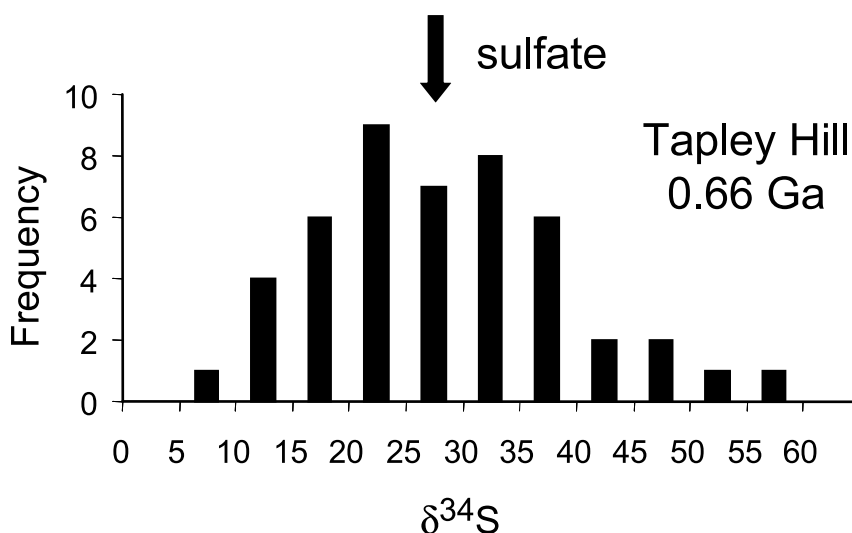
Fig. 5. The frequency of sulfide isotopic compositions is shown for the Neoproterozoic Tapley Hill formation from the Adelaide Rift Complex of Central Australia. Also shown is the isotopic composition of sulfate in anhydrite precipitated within the formation. Data is from Gorjan and others (2000).

Indeed, other processes, as explored below, may well have controlled the isotopic composition of sulfur species.

We consider the Neoproterozoic sulfur cycle further. Despite the preponderance of [34]S-enriched sulfides, a number of sulfides are [34]S depleted compared to sulfate (see fig. 5) indicating a formation pathway through microbial sulfate reduction (for example, Canfield, 2001). However, an equal number are also [34]S enriched compared to sulfate. This situation is not encountered in modern sediments and is rare in the Phanerozoic. Such [34]S-enriched sulfides can be explained by significant pyrite formation in sediments in the zone of sulfate depletion where the δ^{34}S of sulfate increases as [34]S-depleted sulfide is formed by sulfate reduction. This δ^{34}S enrichment of sulfides does not occur today because most pyrite presently forms in the upper sediment layers where sulfate concentrations are not greatly reduced, and hence the δ^{34}S of sulfate does not deviate strongly from the seawater value. Low seawater sulfate concentrations can, however, generate the situation where significant pyrite formation occurs in a zone of strong sulfate depletion, with highly [34]S-enriched sulfate. From diagenetic modeling (see Habicht and others, 2002), histograms of the distribution of sediment pyrite δ^{34}S values are similar to the Tapley Hill Formation with sulfate concentrations in the range of only 200 to 300 μM. Further modeling (Thamdrup and Berg, unpublished) shows that more or less modern sulfur isotope distributions are generated with > 1 mM sulfate. Therefore, very low sulfate concentrations are further indicated during the time of Tapley Hill deposition. This adds to other evidence for low sulfate concentrations, at least in the later Neoproterozoic, based on high frequency fluctuations in the isotopic composition of seawater sulfate. These observations require a small sulfate reservoir with low sulfate concentrations (Hurtgen and others, 2002).

Therefore, at least in the middle to late Neoproterozoic where the sulfur cycle is most out of balance isotopically, very low seawater sulfate concentrations persist with δ^{34}S values in the 20 permil to 30 permil range, from which sulfide forms with a similar average isotopic composition. A problem, then, is identifying where the isotopically
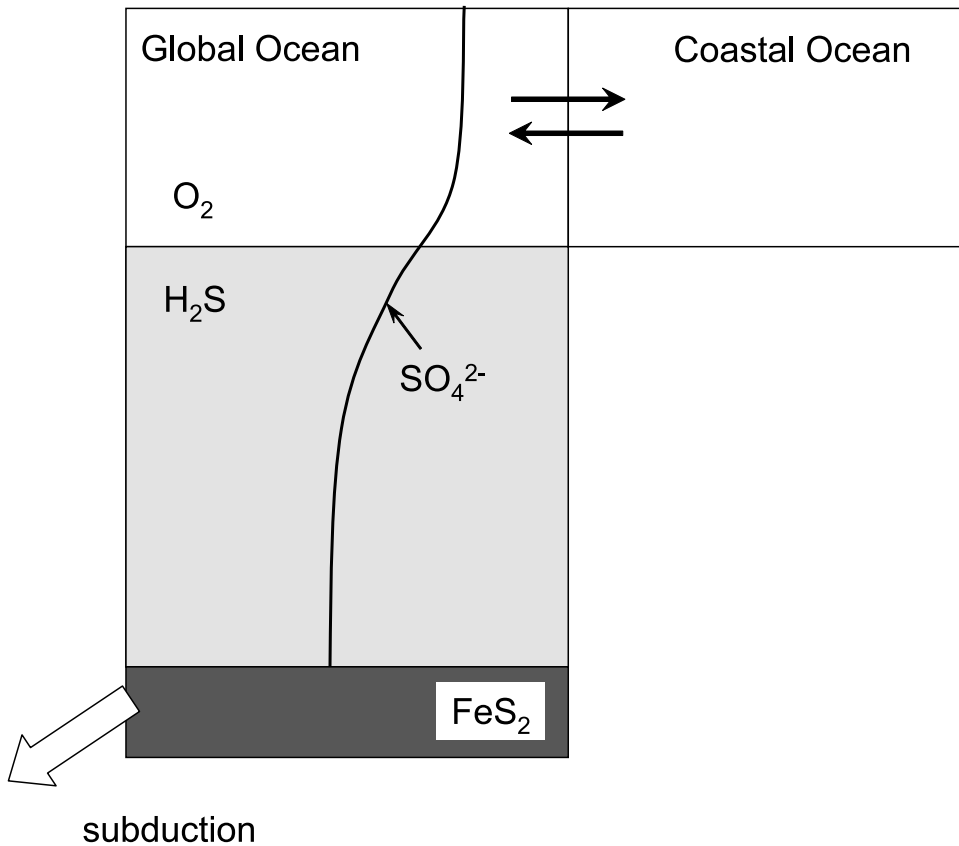
Fig. 6. A simplified cartoon of the Neoproterozoic and Mesoproterozoic sulfur cycle during periods of sulfidic marine bottom water. Low sulfate concentrations, probably in the range of about 300 μM to 2 mM may have experienced a decrease in concentration into the sulfidic bottom waters. Otherwise, the surface ocean probably exchanged sulfate with the coastal ocean with concentrations comparable to the surface ocean, except in restricted basins where the sulfate concentration may have been significantly reduced (see Shen and others, 2002). Pyrite formed from Fe depositing into the deep marine basin would have been mostly subducted, forming an important return route of sulfur from the surface environment into the mantle. See text for details.

depleted sulfide was precipitated assuming sulfur entered the system with an isotopic composition similar to the present crustal average of about 3 permil. Logan and others (1995) suggested that isotopically depleted sulfides may have been precipitated in a sulfidic deep ocean where sulfate was not severely depleted in concentration. In this case, pyrite would form in the water column with an isotopic composition similar to the water column sulfide, as seen in the Black Sea today (Muramoto and others, 1991). These sulfides, depositing mostly in deeper water, would have a low preservation potential, and would be substantially lost by subduction.

Therefore, the history of sulfide preservation provides a probable partial answer to the apparent isotope mass balance problem. Important parts of the isotope record are lost, and indeed, deep water sulfides from the approximately 0.6 Ga Issac Formation and the Kaza Group of the Caribou Mountains, Canada, show much more ^{34}S-depleted sulfides than found in the Tapley Hill Formation. This difference doesn't explain, however, why the apparent isotope imbalance is particularly severe in the late Neopro-

Table 4

Isotopic composition of fluxes into and out of the mantle

Flux	$\delta^{34}S$ ‰
volcanic outgassing	0
hydrothermal input	0
ocean crust weathering	0
hydrothermal sulfate reduction	[a]$\delta^{34}S_{sulfate}$
sediment sulfide subduction	[b]$\Delta_{sulfate\text{-}pyrite}$

[a]isotopic composition of seawater sulfate at a given time
[b]prescribed isotope difference between seawater sulfate and subducted sulfide

terozoic and not throughout the Mesoproterozoic, where the oceans were also believed to have been sulfidic (see above). This issue will be considered in more detail below.

Logan and others (1995) further suggested that the ^{34}S-enriched sulfides preserved could have been formed from the onlapping of sulfate-depleted, and hence ^{34}S-enriched, water onto shelf areas where the pyrites would have formed from sulfate enriched in ^{34}S compared to the ocean mean. They described a sulfate minimum zone somewhat analogous to a modern oxygen minimum zone. The low sulfate concentrations described in the present report would make such an analogy attractive. Low sulfate concentrations are important because it would be difficult under marine conditions to reduce high sulfate concentration (present seawater sulfate is 28 mM) sufficiently to form zones of substantially reduced sulfate concentration enriched in ^{34}S.

There are, however, some potential pitfalls with this hypothesis. Namely, a sulfate minimum zone would form in the anoxic portion of the water column, and any associated ^{34}S-enriched sulfates would also be contained in anoxic water. However, geochemical indicators for the Tapley Hill Formation, for example, show that these sediments were deposited in oxygen-containing bottom water (Gorjan and others, 2000). Furthermore, in the Tapley Hill Formation, preserved sulfates are not particularly ^{34}S-enriched (fig. 5). Therefore, even shallow-water diagenetic sulfides may have formed from sulfate with an isotopic composition representative of the marine reservoir as a whole.

In summary, part of the problem with the sulfur isotope balance in the Neoproterozoic is likely due to deep-water precipitation of ^{34}S-depleted pyrite in a sulfidic ocean, with substantial loss of this pyrite by subduction as suggested by Logan and others (1995) (as explored below, this situation would have initiated in the Paleoproterozoic on transition to sulfidic bottom water conditions). As discussed above, the coastal ocean probably received sulfate in low concentrations with an isotopic composition resembling the surface ocean. A cartoon displaying these aspects of Neoproterozoic ocean chemistry is shown in figure 6. The subduction of ^{34}S-depleted sulfide is another potential influence on the isotopic composition of the surface sulfur reservoir. Indeed, if this subducted pyrite had an isotopic composition different from the average for the reservoir, the isotopic composition of the residual sulfur in the reservoir must change. For example, if the surface reservoir had a $\delta^{34}S$ of 3 permil, and sulfate had a $\delta^{34}S$ of 20 permil, a fractionation of only 20 permil between sulfate and sulfide would produce a $\delta^{34}S$ for sulfide of 0 permil. The subduction of these sulfides would increase the $\delta^{34}S$ of the surface reservoir. A simple model exploring this issue is developed below.
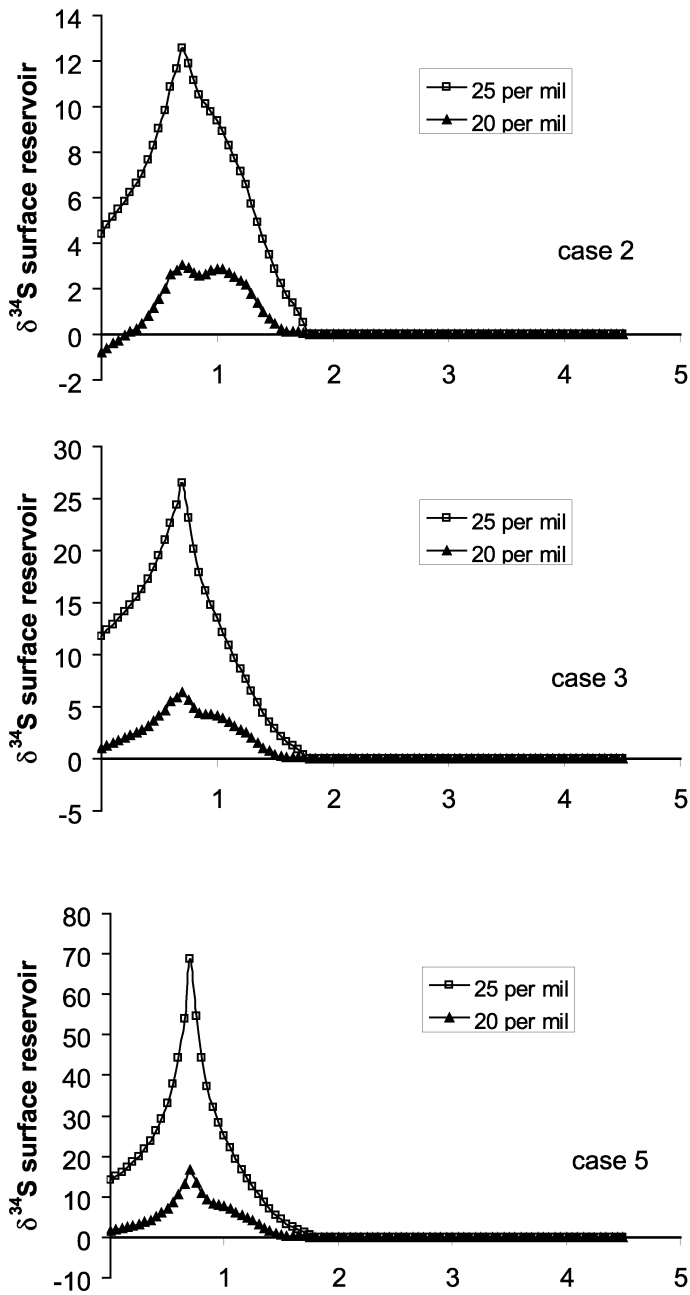
Fig. 7. The evolution of the isotopic composition of the surface sulfur reservoir with the same model cases shown in figure 4, but keeping track of the isotopic compositions of the inputs and outputs to the surface reservoir. These are shown in table 4. The model is run with fractionations between seawater sulfate and suducted sulfide ($\Delta_{\text{sulfate-pyrite}}$) of both 20 ‰ and 25 ‰. See text for details.
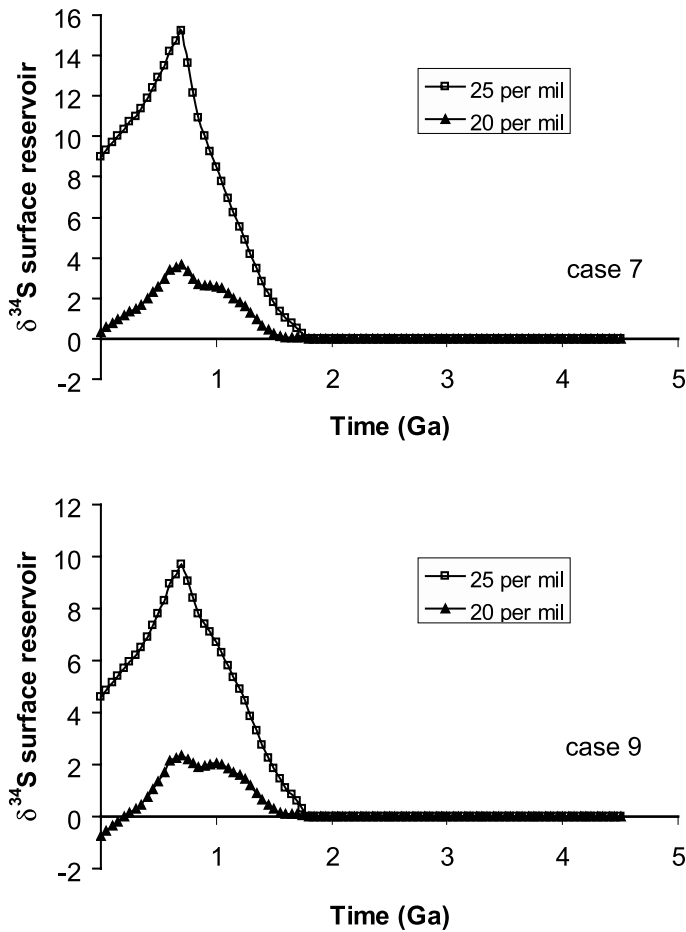
Fig. 7. (*continued*)

Sulfur Isotope Reservoir Model

Each of the sulfur fluxes into and out of the mantle has an associated isotopic composition (table 4). Thus, Earth surface volcanic activity and mid ocean hydrothermal input deliver mantle sulfur to the surface reservoir with a $\delta^{34}S$ of near 0 permil. These inputs may, in fact, give $\delta^{34}S$ values that vary from 0 permil due to the addition of reduced seawater sulfate, as in the case of hydrothermal sulfides, or from sedimentary sulfate, as in the case of volcanoes (see above). However, these extra sulfur sources represent recycled sulfur and are not primary inputs. The sulfide weathered during hydrothermal circulation is added to seawater with a $\delta^{34}S$ of 0 permil, and the sulfate permanently removed during thermochemical sulfate reduction at spreading centers is fixed in the crust with the isotopic composition of the sulfate source (for example, Alt, 1994). Finally, sulfide is subducted with an isotopic composition depending on the fractionation between the sulfate and the sulfide. This is the only free parameter in the model.

The surface reservoir models from figure 4 (see also table 3) were run keeping track of the isotopic composition of the various inputs and outputs. The evolution of the isotopic composition of the surface reservoir for each model is shown in figure 7

with isotope fractionations (Δ^{34}_{SO4}-Δ^{34}_{H2S}) of both 20 permil and 25 permil. These fractionations are probably realistic, if not somewhat low, for a middle-to-late Protero-zoic ocean before the influence of sulfur processing by microbial disproportionation process, which was first expressed at around 0.7 Ga (although these organisms likely evolved much earlier) (Canfield and Teske, 1996). In all cases, the isotopic composi-tion of the surface reservoir is influenced by the subduction of isotopically depleted sulfide into the mantle. If large fractionations are used, the isotopic composition of the surface reservoir is even more affected. If lower fractionations are used, the surface reservoir becomes [34]S-depleted relative to the mantle because sulfide is subducted with a δ^{34}S greater than the crustal average (not shown).

From all the results shown here, the isotopic composition of the surface reservoir can be greatly influenced by the loss of isotopically depleted sulfide due to subduction, even with relatively modest fractionations between sulfate and sulfide of only 20 to 25 permil. Thus, there is the real possibility that the surface reservoir was out of balance isotopically during the Neoproterozoic, contributing to the unusual isotopic distribu-tion of sulfur at this time (fig. 2A). Note that this situation was initiated in the late Paleoproterozoic when sulfidic ocean bottom water first occurred (table 2), but it climaxed in the Neoproterozoic. Furthermore, an isotope imbalance in the surface reservoir could have persisted through much of the Phanerozoic, but is not expressed in the isotope record (fig. 2A) because the average isotopic composition of sulfide falls below the crustal average. Therefore, any imbalance would be impossible to detect from the isotope record alone.

The model results show the possibility, indeed probability, that the isotopic composition of the surface sulfur reservoir has changed through time, particularly when influenced by subduction of [34]S-depleted sulfides. Thus far, the only real constraint on the model is that the isotopic composition of the surface sulfur reservoir cannot exceed the isotopic composition of coeval seawater sulfate. Further constraints could possibly come from the analysis of terrestrial deposits intercepting surface runoff which, on average, should fix pyrite with something near the crustal average isotopic composition. Thus, if the sulfate concentration is low, the isotopic composition of the sulfides formed should approach the isotopic composition of the sulfate from which the sulfides were formed.

SUMMARY AND EXTENSIONS

Through all of Earth history the surface reservoir of sulfur has been in dynamic exchange with the Earth's mantle, and the amount of sulfur accumulating into the surface reservoir has depended on ocean and atmospheric chemistry. Importantly, oxygen has provided a critical control on the sizes and nature of the Earth surface sulfur reservoir. With low atmospheric oxygen levels, the resulting anoxic deep ocean, whether iron rich or sulfide rich, facilitated sulfur delivery back into the mantle. With high atmospheric oxygen levels, and an oxygenated deep ocean, the principal removal pathway for sulfur back into the mantle disappears, and over the last 0.7 Ga, in response to deep-water oxygenation, probably about ½ of the surface reservoir of sulfur has accumulated. The surface reservoir of sulfur is also out of steady-state and, as long as the deep ocean remains oxygen rich, will continue to accumulate sulfur well into the future.

The isotopic composition of the surface reservoir may have deviated from the long-term crustal average due to the subduction of [34]S-depleted sulfides during times of sulfidic ocean water, culminating in the mid to early Neoproterozoic. As a result, the surface reservoir became more [34]S-enriched. An increase in atmospheric oxygen in the late Neoproterozoic oxidized the deep ocean, leading to the accumulation of mantle-derived sulfur in the surface reservoir and a return towards mantle values.

Low concentrations of sulfate are indicated through most of the Precambrian, and surprisingly low concentrations in the late Neoproterozoic. Here, and in the Mesoproterozoic, low sulfate concentrations could have resulted from substantial deposition of sulfide in a dominantly anoxic, sulfidic, ocean. The problem may have become particularly acute in the late Neoproterozoic if the surface reservoir of sulfur was as small as the model results suggest. In this case, a small surface reservoir could have contributed to a smaller supply of sulfur to the oceans by weathering, reducing seawater sulfate concentrations.

There was likely an increase in the size of the surface sulfur reservoir through the Phanerozoic. This increase in reservoir size, combined with increased oxygen levels promoting extensive pyrite weathering and reduced ocean anoxia, contributed to increasing levels of seawater sulfate. The isotope record suggests that the partitioning of sulfur into the sulfate reservoir has increased through the early Phanerozoic, reaching modern proportions only by about 0.3 Ga. This increase in the significance of sulfate burial in evaporates through the Phanerozoic could be a result of increasing sulfate concentrations in the oceans. Indeed, except for a single early Cambrian analysis, fluid inclusion studies indicate low Paleozoic marine sulfate levels of about 10 mM reaching near-modern levels of around 20 mM only by about 0.3 Ga (Horita and others, 2002).

REFERENCES

Alt, J. C., 1994, A sulfur isotopic profile through the Troodos ophiolite, Cyprus: primary composition and the effects of seawater hydrothermal alteration: Geochimica et Cosmochimica Acta, v. 58, p. 1825–1840.
Alt, J. C., and Shanks III, W. C., 1998, Sulfur in serpentinized oceanic peridotites: Serpentinization processes and microbial sulfate reduction: Journal of Geophysical Research, v. 103, p. 9917–9929.
——— 2003, Serpentinization of abyssal peridotites from the MARK area, Mid-Atlantic Ridge: Sulfur geochemistry and reaction modeling: Geochimica et Cosmochimica Acta, v. 67, p. 641–653.
Alt, J. C., Anderson, T. F., and Bonnell, L., 1989, The geochemistry of sulfur in a 1.3 km section of hydrothermally altered oceanic crust, DSDP Hole 504B: Geochimica et Cosmochimica Acta, v. 53, p. 1011–1023.
Alt, J. C., Zuleger, E., and Erzinger, J., 1995, Mineralogy and stable isotopic compositions of the hydrothermally altered lower sheeted dike complex, Hole 504B, Leg 140, *in* Erzinger, J., Becker, K., Dick, H. J. B., and Stokking, L. B., editors, Proceedings of the Ocean Drilling Program, Scientific Results, 137/140: College Station, Texas, Texas A & M University, Ocean Drilling Program, p. 155–166.
Arnold, G. L., Anbar, A. D., Barling, J., and Lyons, T. W., 2004, Molybdenum isotope evidence for widespread anoxia in midproterozoic oceans: Science, v. 304, p. 87–90.
Bach, W., and Edwards, K. J., 2003, Iron and sulfide oxidation within the basaltic ocean crust: Implications for chemolithoautotrophic microbial biomass production: Geochimica et Cosmochimica Acta, v. 67, p. 3871–3887.
Berkner, L. V., and Marshall, L. C., 1965, On the origin and rise of oxygen concentration in the Earth's atmosphere: Journal of Atmospheric Research, v. 22, p. 225–261.
Berner, E. K., and Berner, R. A., 1996, Global Environment: Water, Air, and Geochemical Cycles: Upper Saddle River, New Jersey, Prentice-Hall, Inc., 376 p.
Berner, R. A., and Raiswell, R., 1983, Burial of organic carbon and pyrite sulfur in sediment over Phanerozoic time: a new theory: Geochimica et Cosmochimica Acta, v. 47, p. 855–862.
Berner, R. A., Petsch, S. T., Lake, J. A., Beerling, D. J., Popp, B. N., Lane, R. S., Laws, E. A., Westley, M. B., Cassar, N., Woodward, F. I., and Quick, W. P., 2000, Isotope fractionation and atmospheric oxygen: Implications for Phanerozoic O_2 evolution: Science, v. 287, p. 1630–1633.
Berry, W. B. N., and Wilde, P., 1978, Progressive ventilation of the oceans- an explanation for the distribution of the lower Paleozoic black shales: American Journal of Science, v. 278, p. 257–275.

Bjerrum, C. J., and Canfield, D. E., 2002, Ocean productivity before about 1.9 Gyr ago limited by phosphorus adsorption onto iron oxides: Nature, v. 417, p. 159–162.

Canfield, D. E., 1993, Organic matter oxidation in marine sediments, *in* Wollast, R., Mackenzie, F. T., and Chou, L., editors, Interactions of C, N, P and S Biogeochemical Cycles and Global Change: Berlin, Springer, p. 333–363.

—— 1998, A new model for Proterozoic ocean chemistry: Nature, v. 396, p. 450–453.

—— 2001, Isotope fractionation by natural populations of sulfate-reducing bacteria: Geochimica et Cosmochimica Acta, v. 65, p. 1117–1124.

Canfield, D. E., and Raiswell, R., 1999, The evolution of the sulfur cycle: American Journal of Science, v. 299, p. 697–723.

Canfield, D. E., and Teske, A., 1996, Late Proterozoic rise in atmospheric oxygen concentration inferred from phylogenetic and sulphur-isotope studies: Nature, v. 382, p. 127–132.

de Hoog, J. C. M., Taylor, B. E., and van Bergen, M. J., 2001, Sulfur isotope systematics of basaltic lavas from Indonesia: implications for the sulfur cycle in subduction zones: Earth and Planetary Science Letters, v. 189, p. 237–252.

Elderfield, H., and Schultz, A., 1996, Mid-ocean ridge hydrothermal fluxes and the chemical composition of the ocean, *in* Wetherill, G. W., Albee, A. L., and Burke, K. C., editors: Palo Alto, California, Annual Review of Earth and Planetary Sciences, v. 24, p. 191–224.

Farquhar, J., Bao, H. M., and Thiemens, M., 2000, Atmospheric influence of Earth's earliest sulfur cycle: Science, v. 289, p. 756–758.

Farquhar, J., Savarino, J., Airieau, S., and Thiemens, M. H., 2001, Observation of the wavelength-sensitive mass-dependent sulfur isotope effects during SO_2 photolysis: Implications for the early atmosphere: Journal of Geophysical Research, v. 106, p. 32829–32839.

Farquhar, J., Wing, B. A., McKeegan, K. D., Harris, J. W., Cartigny, P., and Thiemens, M. H., 2002, Mass-independent sulfur of inclusions in diamond and sulfur recycling on early Earth: Science, v. 298, p. 2369–2372.

Garrels, R. M., and Lerman, A., 1981, Phanerozoic cycles of sedimentary carbon and sulfur: Proceedings of the National Academy of Sciences USA, v. 78, p. 4652–4656.

Garrels, R. M., and Perry, Jr., E. A., 1974, Cycling of carbon, sulfur, and oxygen through geologic time, *in* Goldberg, E. D., editor, The Sea: New York, John Wiley and Sons, p. 303–336.

Gorjan, P., Veevers, J. J., and Walter, M. R., 2000, Neoproterozoic sulfur-isotope variation in Australia and global implications: Precambrian Research, v. 100, p. 151–179.

Grotzinger, J. P., and Kasting, J. F., 1993, New constraints on Precambrian ocean composition: Journal of Geology, v. 101, p. 235–243.

Gurnis, M., and Davies, G. F., 1986, Apparent episodic crustal growth arising from a smoothly evolving mantle: Geology, v. 14, p. 396–399.

Habicht, K. S., Gade, M., Thamdrup, B., Berg, P., and Canfield, D. E., 2002, Calibration of sulfate in the Archean ocean: Science, v. 298, p. 2372–2374.

Halmer, M. M., Schmincke, H. U., and Graf, H. F., 2002, The annual volcanic gas input into the atmosphere, in particular into the stratosphere: a global data set for the past 100 years: Journal of Volcanology and Geothermal Research, v. 115, p. 511–528.

Hansen, K. W., and Wallmann, K., 2003, Cretaceous and Cenozoic evolution of seawater composition, atmospheric O_2 and CO_2: A model perspective: American Journal of Science, v. 303, p. 94–148.

Hay, W. W., Sloan, II, J. L., and World, C. N., 1988, Mass/age distribution and composition of sediments on the ocean floor and the global rate of sediment subduction: Journal of Geophysical Research, v. 93, p. 14933–14940.

Hayes, J. M., Lambert, I. B., and Strauss, H., 1992, The sulfur-isotopic record, *in* Schopf, J. W., and Klein, C., editors, The Proterozoic Biosphere: A multidisciplinary study: Cambridge, Cambridge University Press, p. 129–132.

Hoffman, P. F., Kaufman, A. J., Halverson, G. P., and Schrag, D. P., 1998, A Neoproterozoic snowball Earth: Science, v. 281, p. 1342–1346.

Holland, H. D., 1973, Systematics of isotopic composition of sulfur in oceans during Phanerozoic and its implications for atmospheric oxygen: Geochimica et Cosmochemica Acta, v. 37, p. 2605–2616.

—— 1984, The Chemical Evolution of the Atmosphere and Oceans: Princeton Series in Geochemistry: Princeton, New Jersey, Princeton University Press, 582 p.

—— 1994, Early Proterozoic atmospheric change, *in* Bengston, S., editor, Early Life on Earth: New York, Columbia University Press, p. 237–244.

Holser, W. T., Schidlowski, M., Mackenzie, F. T., and Maynard, J. B., 1988, Geochemical cycles of carbon and sulfur, *in* Gregor, C. B., Garrels, R. M., Mackenzie, F. T., and Maynard, J. B., editors, Chemical Cycles in the Evolution of the Earth: New York, John Wiley and Sons, p. 105–173.

Horita, J., Zimmermann, H., and Holland, H. D., 2002, Chemical evolution of seawater during the Phanerozoic: Implications from the record of marine evaporites: Geochimica et Cosmochimica Acta, v. 66, p. 3733–3756.

Hurtgen, M. T., Arthur, M. A., Suits, N. S., and Kaufman, A. J., 2002, The sulfur isotopic composition of Neoproterozoic seawater sulfate: implications for a snowball Earth?: Earth and Planetary Science Letters, v. 203, p. 413–429.

Isley, A. E., and Abbott, D. H., 1999, Plume-related mafic volcanism and the deposition of banded iron formation: Journal of Geophysical Research, v. 104, p. 15461–15477.

Jørgensen, B. B., 1982, Mineralization of organic matter in the sea bed - the role of sulfate reduction: Nature, v. 296, p. 643–645.

Kasasaku, K., Minari, T., Mukai, H., and Murano, K., 1999, Stable isotope ratios of the gases from Mt.

Sakurajima and Satsuma-Iwojima volcanoes- Assessment of volcanic sulfur on rainfall sulfate in Kagoshima Prefecture: Nippo Kagaku Kaishi, v. 7, p. 479–486.

Knoll, A. H., 1992, Biological and biogeochemical preludes to the Ediacaran radiation, *in* Lipps, J. H., and Signor, P. W., editors, Origin and Early Evolution of the Metazoa: New York, Plenum Press, p. 53–84.

Logan, G. A., Hayes, J. M., Hieshima, G. B., and Summons, R. E., 1995, Terminal Proterozoic reorganization of biogeochemical cycles: Nature, v. 376, p. 53–56.

Muramoto, J. A., Honjo, S., Fry, B., Hay, B. J., Howarth, R. W., and Cisne, J., L., 1991, Sulfur, iron and organic carbon fluxes in the Black Sea: sulfur isotopic evidence for origin of sulfur fluxes: Deep- Sea Research, v. 38, p. S1151–S1187.

Pavlov, A. A., and Kasting, J. F., 2002, Mass-independent fractionation of sulfur isotopes in Archean sediments: Strong evidence for an anoxic Archean atmosphere: Astrobiology, v. 2, p. 27–41.

Poulton, S. W., Fralick, P. W., and Canfield, D. E., 2004, The transition to a sulphidic ocean ~1.84 billion years ago: Nature, v. 431, p. 173–177.

Raiswell, R., and Canfield, D. E., 1998, Sources of iron for pyrite formation in marine sediments: American Journal of Science, v. 298, p. 219–245.

Sakai, H., Casadevall, T. J., and Moore, J. G., 1982, Chemistry and isotope ratios of sulfur in basalts and volcanic gases at Kilauea Volcano, Hawaii: Geochimica et Cosmochimica Acta, v. 46, p. 729–738.

Schlesinger, W. H., 1997, Biogeochemistry: An analysis of global change: San Diego, Academic Press, 588 p.

Shanks, W. C., III, and Seyfried, W. E., Jr., 1987, Stable isotope studies of vent fluids and chimney minerals, southern Juan de Fuca Ridge: sodium metasomatism and seawater sulfate reduction: Journal of Geophysical Research, v. 92, p. 11,387–11,399.

Shen, Y., Canfield, D. E., and Knoll, A. H., 2002, Middle Proterozoic ocean chemistry: Evidence from the McArthur Basin, Northern Australia: American Journal of Science, v. 302, p. 81–109.

Shen, Y., Knoll, A. H., and Walter, M. R., 2003, Evidence for low sulphate and anoxia in a mid-Proterozoic marine basin: Nature, v. 423, p. 632–635.

Stoiber, R. E., Williams, S. N., and Huebert, B., 1987, Annual contribution of sulfur dioxide to the atmosphere by volcanoes: Journal of Volcanology and Geothermal Research, v. 33, p. 1–8.

Strauss, H., 1993, sulfur isotope record of Precambrian sulfate: new data and a critical evaluation of the existing record: Precambrian Research, v. 63, p. 225–246.

Turcotte, D. L., 1980, On the thermal evolution of the Earth: Earth and Planetary Science Letters, v. 48, p. 53–58.

Von Damm, K. L., 1990, Seafloor hydrothermal activity: Black smoker chemistry and chimneys: Annual Review of Earth and Planetary Science, v. 18, p. 173–204.

von Huene, R., and Scholl, D. W., 1991, Observations at convergent margins concerning sediment subduction, subduction erosion, and the growth of continental crust: Reviews of Geophysics, v. 29, p. 279–316.